SELF-SIMILAR CHARGE TRANSMISSION IN GAPPED GRAPHENE

Article *in* Fractals · April 2016

Impact Factor: 1.22 · DOI: 10.1142/S0218348X16300026

4 authors:

D. S. Díaz-Guerrero

Universidad Autónoma del Estado de Morelos

10 PUBLICATIONS **7** CITATIONS

SEE PROFILE

Isaac Rodríguez-Vargas

Autonomous University of Zacatecas

64 PUBLICATIONS **186** CITATIONS

SEE PROFILE

Gerardo G. Naumis

Universidad Nacional Autónoma de México

136 PUBLICATIONS **1,010** CITATIONS

SEE PROFILE

L.M. Gaggero Sager

Universidad Autónoma del Estado de Morelos

93 PUBLICATIONS **479** CITATIONS

SEE PROFILE

Fractals, Vol. 24, No. 2 (2016) 1630002 (8 pages)

DOI: 10.1142/S0218348X16300026

SELF-SIMILAR CHARGE TRANSMISSION IN GAPPED GRAPHENE

D. S. DÍAZ-GUERRERO,* I. RODRÍGUEZ-VARGAS,†
G. G. NAUMIS‡ and L. M. GAGGERO-SAGER*,§
*Instituto de Investigación en Ciencias Básicas y Aplicadas
Universidad Autónoma del Estado de Morelos, Cuernavaca Morelos, Mexico
†Unidad de Física, Universidad Autónoma de Zacatecas, Zacatecas ZAC, Mexico
‡Instituto Física, Departamento de Física-Química
Universidad Nacional Autónoma de Mexico (UNAM)
Apdo. Postal 20-364, 01000, Mexico DF, Mexico
§lgaggero@uaem.mx

Received August 9, 2015
Accepted February 1, 2016
Published April 26, 2016

Abstract

A new self-similar multibarrier system is proposed and used to study transmission of Dirac electrons in graphene. Such system is based on the scaling of the length and energy of the barriers. The use of self-similar structures allows us to compare the transmission in graphene and gallium arsenide (GaAs). The transmission coefficient for charge carriers in graphene shows a surprising scaling behavior structure, which is not seen in GaAs. The scaling properties are established as a function of three parameters: barrier's energy, the length and the generation of the system.

Keywords: Self-Similar; Graphene; Transport Electronics.

§Corresponding author.

1. INTRODUCTION

Graphene[1] is considered as one of the most promising new materials. This first truly two, dimensional crystal[2] has impressive physical properties, such as ballistic transport and sustainable currents up to ($10^8\,\mathrm{A/cm^2}$).[1,3] As a consequence, graphene is not only important from a technological point of view, but also is considered as an inflexion point in quantum physics. For instance, charge carriers in graphene follow an effective quantum relativistic (Dirac) equation instead of the usual Schrödinger's equation for traditional materials. This leads to new effects, like the scattering produced by external potentials or impurities is different from what is observed in ordinary materials.[4–6] Charge carriers can be transmitted perfectly due to the Klein effect, opposite to what happens in non-relativistic materials where there is no perfect transmission and substitutional impurities can produce multifractal states.[7,8] Thus, a whole new world is open to investigate the possible effects of external potential geometries, which can be imposed to graphene by different means, for example, using certain type of substrates, strain, electrostatic gates, impurities, electromagnetic fields, etc.[9,10]

For applications, an important issue is how to engineer substrate-induced bandgap opening in epitaxial graphene,[10] allowing to investigate how different multibarrier geometries affect the properties of graphene. Among the possible geometries, self-similarity has a paramount importance, since scale invariance is a fundamental property of many natural phenomena, as can be seen in reports that ranges from the distribution and abundance of species, temporal occurrence of earthquakes, and even in the growth of complex networks and trees.[11–14] From the technological standpoint, self-similarity can also be exploited to produce useful devices.[15–17] Particularly, photoconductive fractal antennas show an efficient multiband emission of terahertz radiation owing to the self-similarity of the fractal structure.[16] Despite that, self-similar structures are getting plenty of attention,[18] only a handful of experiments confirms a self-similar behavior in its physical properties.[19–21] Likewise, many theoretical works claim that physical properties, such as transmission or reflection probabilities, display self-similarity. Unfortunately, most of them are just a matter of visual perception, although there are some significantly important papers where the scaling properties are discussed such as Refs. 22–24. Even in the case of quasicrystals, which are considered as one of the archetypal examples of self-similar structures, it has been elusive to find the scaling properties of the corresponding physical properties.[25,26]

2. METHODS

First, we define a novel self-similar multibarrier structure in graphene in which the main physical property, namely charge transport, presents a surprising self-similar pattern. To build our multibarrier structure in one direction (the x-axis), we implement a variant of the middle-third Cantor set construction[27] using square barriers as indicated in Fig. 1. We begin with a line-segment of length Lt,

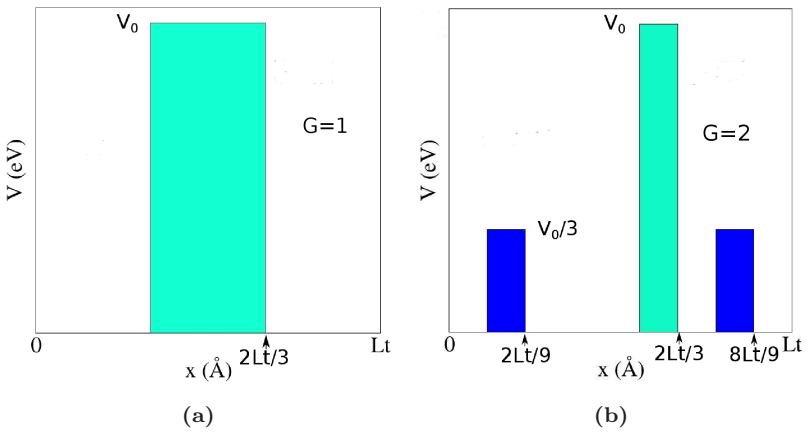

Fig. 1 Potential construction. First four generations ($G = 1, 2, 3, 4$) of the multibarrier potential. Each barrier is scaled (by a factor of 1/3) in its width, and so the barrier width is 1/3 Lt. The barriers added in the last iteration are scaled in its height. For example, the height of the green ones are one-third of the height of the blue ones. The zooms in $G = 3$ and $G = 4$ illustrate how the potential resembles a previous generation after an appropriate rescaling.

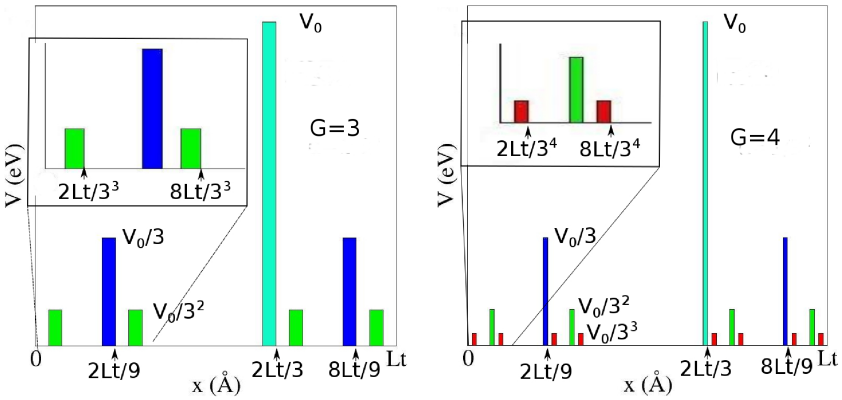

(c) (d)

Fig. 1 (*Continued*)

we divide it in thirds and put a rectangular barrier of energy V_0 in the middle third (its width is Lt/3). We call this the generation one ($G = 1$). The second step consists in taking the remaining line-segments, divide them into thirds and place in their corresponding middle-thirds' scaled copies of the existing barrier. We scale the height and width of the barrier by a scaling factor of 1/3. Additionally, the existing barrier is also scaled in its width by the same factor. Since scaling is a contraction transformation, each scaled barrier copy will have a unique fixed point (*see the fixed point theorem in metric spaces*[28]). By fixed point, we meant an element of the function's domain that is mapped to itself by the function, the scaling function in this case. In the potential construction, this point is a fixed side of each barrier, which will be chosen as the right-hand side. Thus, every successive iteration (generation G) of the structure is obtained by repeating the second step of the construction for the remaining line-segments, using as the "existing barrier" those added in the last iteration, as shown in Fig. 1.

This potential can be described as follows. The Gth generation of the potential consists of $N_G = 2^G - 1$ barriers; the corresponding barriers (those in the Gth iteration) has a width $W_G = \mathrm{Lt}/3^G$ and energy (height) $V_G = V_0/3^{G-1}$. Since the construction of the multibarrier structure is based on the length-scaling of the previous generation barriers, and the addition of energy-scaled new barriers, we search for relations between transmission curves corresponding to different generations of the multibarrier structure. So, we fix the total length of the structure, denoted by Lt (in this case, we use the value of $\mathrm{Lt} = 3500\,\text{Å}$) and the height of the main barrier, denoted by V_0 (using the value of $V_0 = 1\,\mathrm{eV}$).

The self-similar potential does not depend on the perpendicular direction (y-axis), i.e. $V(x, y) = V(x)$ and can be adapted to graphene[1,29–31] by means of symmetry breaking substrates,[32–34] by gated graphene or in other systems, like optical analogies, with a linear spectrum.[35–37]

For graphene, we use the Viana-Gomes *et al.* formalism[33] to compute the transmission coefficient of electrons in gapped graphene. The Hamiltonian for the Dirac electrons under a potential $V(x)$ is given by

$$H = v_F \sigma \cdot \mathbf{p} + \sigma_z V(x), \tag{1}$$

where $V(x) = m(x)v_F^2$ if $x = [x_1, x_2]$ and zero in other case. $V(x)$ defines the region where there is a mass term (q-region) and where carriers are massles Dirac fermions (k-region). The first term of the Hamiltonian is just the Dirac equation used to describe electrons in graphene, where v_F is the Fermi velocity, σ the set of Pauli matrices and $\mathbf{p}$ the moment. For normal incidence on the x-direction, the corresponding wave functions are[33]

$$\psi_k^{\pm}(x) = \frac{1}{\sqrt{2}} \begin{pmatrix} 1 \\ u_{\pm} \end{pmatrix} e^{\pm i k_x x} \tag{2}$$

and

$$\psi_q^{\pm}(x) = \frac{1}{\sqrt{2}} \begin{pmatrix} 1 \\ v_{\pm} \end{pmatrix} e^{\pm i q_x x}, \tag{3}$$

where $u_{\pm} = \pm\mathrm{sign}(E)$ and $v_{\pm} = \frac{E - V(x)}{\hbar v_F(\pm q_x - i k_y)}$. Using these equations, one establishes the continuity conditions when the wave goes from the k-region to the q-region.

With the potential described in Fig. 1 at hand, we compute the transmission coefficient defined as

$$T_G(E) = \frac{|\psi_k^+(\mathrm{Lt})|^2}{|\psi_k^+(0)|^2}. \quad (4)$$

In order to obtain the $\psi_k^+(\mathrm{Lt})$, it is necessary to compute the wave functions, under their respective continuity conditions, corresponding to each one of the $2^G - 1$ q-regions and of the 2^G k-regions. Although in other physical systems it has obtained deep results in closely related geometries,[39] the key difference with the system proposed here is the number of barrier heights. Hence, the only way to do it is by means of a numerical simulation, and in this case using the transfer matrix formalism.[33,38,40] The transfer matrix can be obtained from the continuity conditions of the wave functions in each region of the self-similar structure, the first continuity condition takes place when the wave goes from k_0-region to q_0-region and the second condition when it goes from the q_0-region to k_1-region, and so on. From this, we extract the transmission coefficient for a given energy at the time (see, for instance, Refs. 33 and 38) and then we compute all again for several values of the energy.

3. RESULTS AND DISCUSSION

In Fig. 2a, we show the transmission curves corresponding to generations 6 and 7 of the potential, denoted by $T_6(E)$ and $T_7(E)$, respectively (normal incidence is used in this work). As we can see, it is qualitatively clear that they are related by some kind of transformation. This transformation turns out to be $T_6(E) = [T_7(E)]^9$, where the subindex

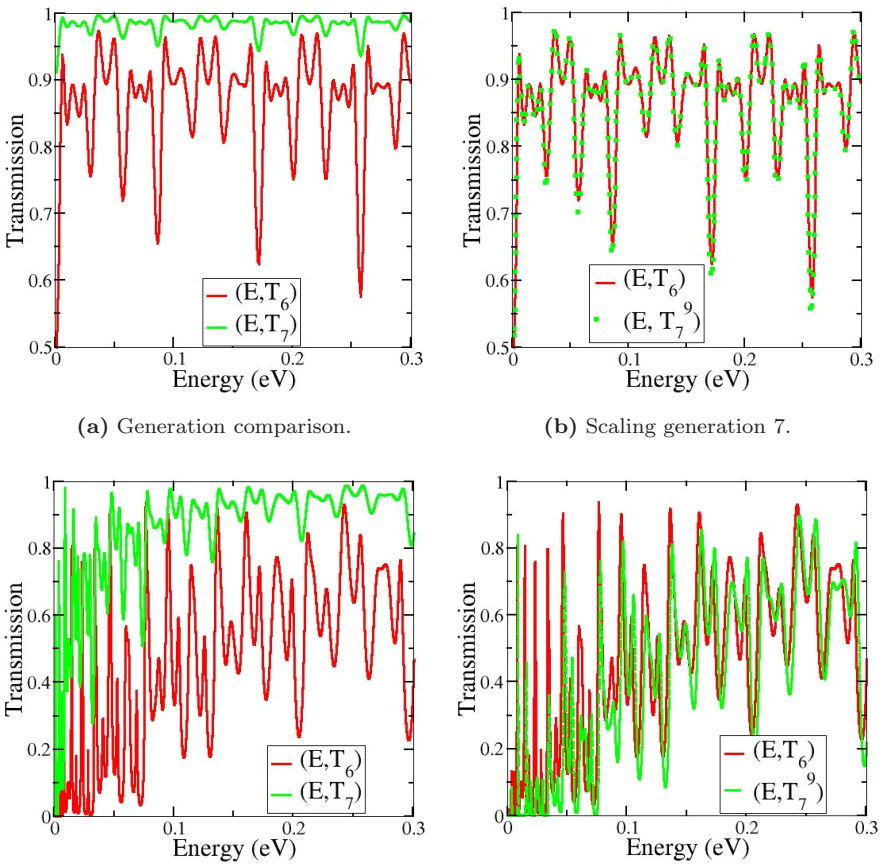

(a) Generation comparison. **(b)** Scaling generation 7.

(c) Comparison GaAs case. **(d)** Scaling generation 7, GaAs case.

Fig. 2 Transmission coefficient scaling for different generations. **(a)** Transmission as a function of energy for the sixth ($G = 6$ the one in red) and seventh ($G = 7$ the one in green) generation of multibarrier graphene using the parameters $V_0 = 1.0\,\mathrm{eV}$ and $\mathrm{Lt} = 3500$ Å. It is worth to note that the inclusion of the $2^{G-1} = 2^6$ barriers of energy $V_0/3^6 \approx 1.37\,\mathrm{meV}$ clearly change the transmission curve overall behavior as can be seen in panel (a). **(b)** Scaled transmission for $G = 6$ and $G = 7$. The scaling transformation is given by the power law Eq. (5), which gives an excellent agreement of the curves. In **(c)** and **(d)**, the transmission and scaled transmission respectively are presented for the same potential but for a typical semiconductor which follows the Schrödinger equation. No self-similar scaling is observed.

stands for the generation number, as seen in Fig. 2b. Thus, $T_6(E)$ are $T_7(E)$ scaled by a single exponent. As may be expected, other bigger generations also follow the same rule. More formally

$$T_G(E) \approx [T_{G+1}(E)]^9, \tag{5}$$

where $G \geq 6$ and G stands for the generation number. This means that any two transmission curves that differ only in the generation of their corresponding potential, are related by some power of the form 9^m, where m is the difference between the generations. To highlight the difference with a typical semiconductor ruled by Schrödinger's equation, in Figs. 2c and 2d, we present the transmission calculated for the same potential generations using $Al_xGa_{1-x}As/GaAs$, instead of graphene. In such system, the energy (height) of the quantum barriers are controlled by the Aluminium concentration.

So far, we have found a scaling between transmission curves that correspond to different generations of the potential, but it seems possible to extend the search for scaling features to other parameters. We have two options at hand, the energy of the starting barrier (V_0) and the total length of the structure (Lt).

Let us explore now another option in our search for scaling features, that is, we take a fixed generation of the potential, say generation 6, and make the calculation for two starting energies. Let us take $V_0 = 0.5\,\text{eV}$ and $V_0 = 1.0\,\text{eV}$. In this case, the form of the curves seen in Fig. 3a, resembles those corresponding to a change in the generation of the potential. Due to the resemblance of these curves with the

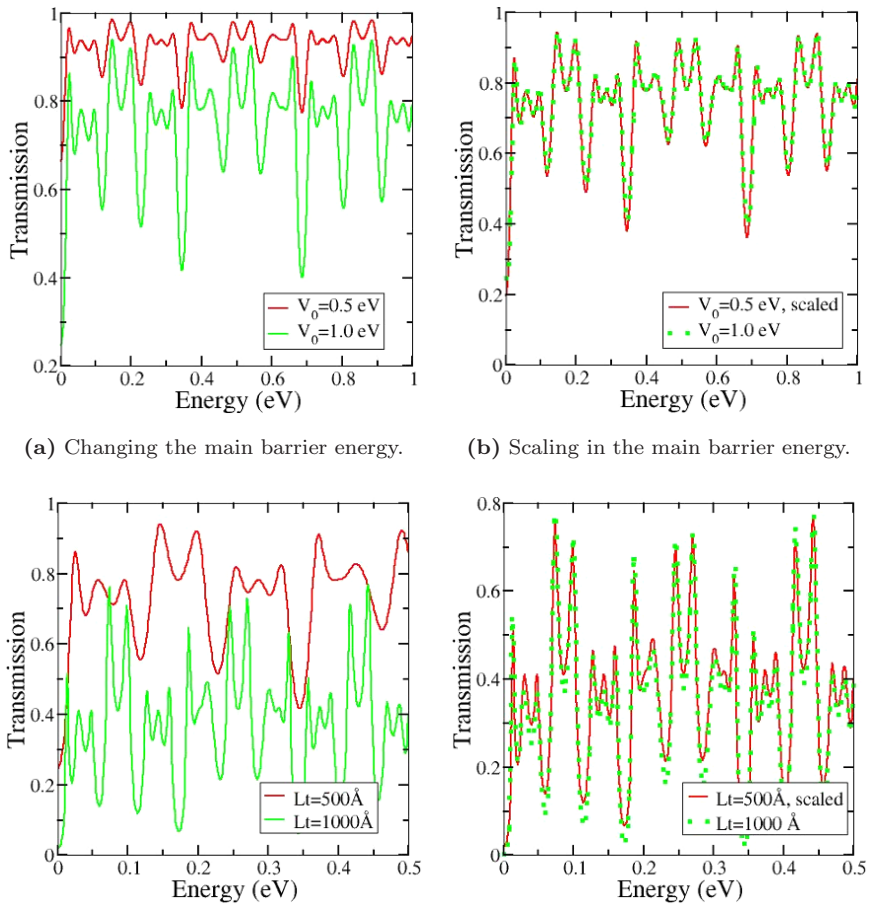

(a) Changing the main barrier energy.

(b) Scaling in the main barrier energy.

(c) Changing the total length.

(d) Scaling in the total length.

Fig. 3 Scaling between barrier energy. **(a)** Comparison between transmission curves for different values of V_0 using generation 6. This case corresponds to the transmission for two potentials with different heights of the main barrier, in this case $V_0 = 0.5\,\text{eV}$ and $V_0 = 1.0\,\text{eV}$. All other parameters are equal. **(b)** Comparison between the scaled plots of **(a)**. The scaling consists in raising $V_0 = 0.5\,\text{eV}$ to the fourth power. **Scaling between lengths. (c)** Comparison between the transmission curves for different lengths (Lt). In this case it is quite clear that the scaling cannot be just raising one curve to a certain power. **(d)** Scaling of the curve with length Lt = 500 Å. This scaling is made of two parts, raising the curve to the fourth power and multiplying its energy by two.

ones of changing generations, we try the same kind of transformation but with a different power.

In this case, one has to raise the curve corresponding to $V_0 = 0.5\,\text{eV}$ to the fourth power to get the one corresponding to $V_0 = 1.0\,\text{eV}$, see Fig. 3b. We determine that the transformation is $T_{1.0}(E) \approx T_{0.5}(E)^4$, where the subindex stands for the V_0 value of the respective structure. In fact, this scaling behavior is more general, i.e.

$$T_{\frac{1}{k}V_0}(E)^{k^2} \approx T_{V_0}(E). \tag{6}$$

Finally, we compare curves corresponding to different lengths of the whole structure, denoted by Lt. Although nothing suggests scaling in this variant at all, see Fig. 3c, our previous results encourage us to a keep searching, but with different transformations. Looking at the mentioned comparison, it seems to be involved in a contraction or a dilation of the x-axis for one of the curves, in addition to the transformation in the transmission. So, we get

$$T_{\frac{1}{\alpha}\text{Lt}}\left(\frac{1}{\alpha}E\right)^{\alpha^2} \approx T_{\text{Lt}}(E), \tag{7}$$

where α represents the value by which the total lengths are related. For instance, if $\alpha = 2$ then we would get $T_{\frac{1}{2}\text{Lt}}(\frac{1}{2}E)^{2^2} \approx T_{\text{Lt}}(E)$, and setting $\text{Lt} = 3500$ this is $T_{1750}(\frac{1}{2}E)^4 \approx T_{3500}(E)$. With this scaling rule applied to the curve corresponding to $\text{Lt} = 1000\,\text{Å}$, a very good approximation is obtained, see Fig. 3d.

Combining expressions (5)–(7), it is possible to get a good approximation to almost every curve that results from the combination of parameters. To do this, all the parameters and the variable E will be arguments of T. Let $\omega = (E, G, V_0, \text{Lt})$ and $\omega' = (\alpha E, G - m, \frac{1}{k}V_0, \alpha\text{Lt})$. That is, ω and ω' are related by a combination of scaling factors. Hence, we get

$$T(\omega) \approx T(\omega')^{9^m k^2/\alpha^2} \tag{8}$$

for $G - m \geq 6$ (for lower values there is no evident scaling between transmission curves).

The scaling relation suggests that the transmission curves follow a scaling rule which is a signature of the self-similar phenomena. In fact, we are in presence of the first true self-similar physical property of graphene. Moreover, even for perfect fractals it is known that the physical properties usually follow a multifractal behavior[26,41] but here only one single scaling exponent is obtained. It is important to remark that in this kind of structures there are always finite size effects due to the break in the scaling of the potential, which affects the first generations. In this particular case, one cannot extend self-similarity beyond the length of the system.

For low generations, the transmittance is basically dominated by the biggest energy barrier. Between $G = 5$ and $G = 6$, there is a dramatic change in the behavior since now the system has transmittance for energies lower than the main barrier height. As generations increase, scaling appears. Generation 6 is the crossover of the geometrical finite size effects in the potential, since they disappear after it. Also, it is clear that in real systems there is also another finite size effect at the bottom of the hierarchy, where the Dirac approach cannot be made due to the rapid variation of the potential at atomic distances.

The approximations obtained are quite useful to predict the transmission as function of the parameters, but it is necessary to measure the degree of matching between curves. So, we calculate the root mean square of the difference between the target curve and the scaled one, we call it drms. For parameter G (scaling between generations of the potential, see Fig. 2b the drms is 5.50×10^{-5}; for V_0 (scaling in the energy of the main barrier, see Fig. 3b the drms is 2.05×10^{-4}; at last for Lt (scaling in the total length of the multibarrier structure, see Fig. 3d the drms is 1.43×10^{-3}. From this, it is quite clear that the better approximation is for the scaling between generations.

This lead us to examine a wider range of energy and check our scaling-laws values. An analysis of the results, shows that the fit is excellent for small energies but tends to decrease in quality as the energy increases, as one should expect in the limiting case of very high energies. Also, the error tends to grow for small transmittance energies. However, if the error is computed for bigger generations, for example, for $G = 7$ against scaled $G = 8$, then the error decreases in a dramatic way, as expected for a good scaling relation. The drms for the Schrödinger case does not reduce as the generations grow, suggesting the absence of a true scaling feature.

The numerical results presented above suggests that this type of potential indeed shows scaling properties, although this scaling is not found in a single curve, but between curves corresponding to different parameters. This is a very interesting result because in fact the transmission coefficient is an intricate combination of the wave functions,

and even more, for a multibarrier potential it is the result of the product of several transfer matrices. This suggests that the wave function have self-similar properties. This is the affirmation in the Gaggero–Pujals theorem[42] for non-relativistic electrons. Thus, it seems plausible that an extension of that theorem could be established for relativistic equations. Another important possibility is to study the non-perpendicular incidence, since Klein tunneling is ruled out in this case.[43]

4. CONCLUSION

In conclusion, the self-similar potential proposed here show various kinds of scaling properties in the transmission curves. This scaling properties gave the possibility to obtain, given a transmission curve and its set of parameters, an almost perfect approximation of the curve corresponding to certain transformation of the original parameters, see (8). It is also suggested that the scaling properties of the transmission curves are drastically affected by the mix of two geometric symmetries, for example, reflectional symmetry and self-similarity, see Refs. 42 and 44.

It is important to address that for a given generation G there is $2^G - 1$ barriers each of which adds a matrix to the overall product. And due to the scaling in the added barriers energy, it is not yet possible to make a rigorous mathematical proof of the scaling properties for the transmission curves, although indeed it is quite compelling and is part of our ongoing research work.

Finally, we found that three ingredients are needed in order to obtain a single scaling of the transmittance, a *self-similar multibarrier system*, *non-reflectional symmetric and quantum relativistic equations*, since the non-relativistic version does not display scaling. A possible heuristic explanation for such phenomena lies in the linear energy–momentum dispersion relation of the Dirac equation, but we save this for a future work.

ACKNOWLEDGMENTS

The authors thank *Consejo Nacional de Ciencia y Tecnología* (CONACYT) for their support.

REFERENCES

1. K. S. Novoselov *et al.*, Electric field effect in atomically thin carbon films, *Science* **306** (2004) 666–669.
2. K. S. Novoselov *et al.*, Two-dimensional atomic crystals, *Proc. Natl. Acad. Sci. USA* **102** (2005) 10451–10453.
3. A. A. Balandin *et al.*, Superior thermal conductivity of single-layer graphene, *Nano Lett.* **8** (2008) 902–907.
4. A. K. Geim and K. S. Novoselov, The rise of graphene, *Nat. Mater.* **6** (2007) 183–191.
5. K. S. Novoselov, Nobel lecture: Graphene: Materials in the flatland, *Rev. Mod. Phys.* **83** (2011) 837–849.
6. D. A. Stone, C. A. Downing and M. E. Portnoi, Searching for confined modes in graphene channels: The variable phase method, *Phys. Rev. B* **86** (2012) 075464.
7. G. G. Naumis, R. A. Barrio and C. Wang, Effects of frustration and localization of states in the Penrose lattice, *Phys. Rev. B* **50** (1994) 9834–9842.
8. G. G. Naumis, C. Wang and R. A. Barrio, Frustration effects on the electronic density of states of a random binary alloy, *Phys. Rev. B* **65** (2002) 134203.
9. A. H. C. Neto *et al.*, The electronic properties of graphene, *Rev. Mod. Phys.* **81** (2009) 109–162.
10. G. Giovannetti *et al.*, Substrate-induced band gap in graphene on hexagonal boron nitride: *Ab initio* density functional calculations, *Phys. Rev. B* **76** (2007) 073103.
11. A. Corral, Long-term clustering, scaling, and universality in the temporal occurrence of earthquakes, *Phys. Rev. Lett.* **92** (2004) 108501.
12. C. Eloy, Leonardos rule, self-similarity, and wind-induced stresses in trees, *Phys. Rev. Lett.* **107** (2011) 258101.
13. J. Harte *et al.*, Self-similarity in the distribution and abundance of species, *Science* **284** (1999) 334–336.
14. C. Song *et al.*, Origins of fractality in the growth of complex networks, *Nat. Phys.* **2** (2006) 275–281.
15. H. Ding *et al.*, Multi-splitting and self-similarity of band gap structures in quasi-periodic plates of Cantor series, *Appl. Phys. Lett.* **100** (2012) 083501.
16. F. Miyamaru *et al.*, Emission of terahertz radiations from fractal antennas, *Appl. Phys. Lett.* **95** (2009) 221111.
17. M. Sun *et al.*, Transmission properties of dual-band cross-dipole fractal slit arrays for near- and mid-infrared wavelengths, *Phys. Rev. B* **74** (2006) 193404.
18. E. Maciá, The role of aperiodic order in science and technology, *Rep. Prog. Phys.* **69** (2006) 397.
19. A. V. Lavrinenko *et al.*, Propagation of classical waves in nonperiodic media: Scaling properties of an optical Cantor filter, *Phys. Rev. E* **65** (2002) 036621.
20. B. Hou *et al.*, Diffraction by an optical fractal grating, *Appl. Phys. Lett.* **85** (2004) 6125.
21. J. O. Estevez *et al.*, Experimental realization of the porous silicon optical multilayers based on the 1-s sequence, *J. Appl. Phys.* **111** (2012) 013103.

22. Y. Sakurada *et al.*, Scaling properties of the Fresnel diffraction field produced by one-dimensional regular fractals, *Pure Appl. Opt.* **3** (1994) 371–380.
23. C. Casanova *et al.*, Self-similar focusing with generalized devil's lenses, *J. Opt. Soc. Am. A* **28** (2011) 210–213.
24. J. C. Castro-Palacio, Self-similar behavior in semiconductor superlattices, *Fractals* **20** (2012) 89–95.
25. G. G. Naumis and J. L. Aragon, Substitutional disorder in a Fibonacci chain: Resonant eigenstates and instability of the spectrum, *Phys. Rev. B* **54** (1996) 15079.
26. R. Nava *et al.*, Perfect light transmission in Fibonacci arrays of dielectric multilayers, *J. Phys., Condens. Matter* **21** (2009) 155901.
27. G. Cantor, Ueber unendliche, lineare punktmannichfaltigkeiten, *Math. Ann.* **21** (1883) 545–591.
28. T. M. Apostol, *Mathematical Analysis* (Addison-Wesley, 1983), p. 92.
29. K. S. Novoselov *et al.*, Two-dimensional gas of massless Dirac fermions in graphene, *Nature* **438** (2005) 197–200.
30. Y. Zhang *et al.*, Experimental observation of the quantum Hall effect and Berry's phase in graphene, *Nature* **438** (2005) 201–204.
31. C. W. Beenakker *et al.*, Quantum goos–Hänchen effect in graphene, *Phys. Rev. Lett.* **102** (2009) 146804.
32. V. H. Nguyen *et al.*, Resonant tunneling structures based on epitaxial graphene on SiC, *Semicond. Sci. Technol.* **26** (2011) 125012.
33. J. V. Gomes and N. M. R. Peres, Tunneling of Dirac electrons through spatial regions of finite mass, *J. Phys., Condens. Matter* **20** (2008) 325221.
34. S. Y. Zhou *et al.*, Substrate-induced bandgap opening in epitaxial graphene, *Nat. Mater.* **6** (2007) 770–775.
35. V. V. Cheianov *et al.*, The focusing of electron flow and a veselago lens in graphene p–n junctions, *Science* **315** (2007) 1252.
36. R. R. Hartmann *et al.*, Smooth electron waveguides in graphene, *Phys. Rev. B* **81** (2010) 245431.
37. R. R. Hartmann and M. E. Portnoi, Quasi-exact solution to the Dirac equation for the hyperbolic-secant potential, *Phys. Rev. A* **89** (2014) 012101.
38. I. Rodríguez-Vargas *et al.*, Resonant tunneling through double barrier graphene systems: A comparative study of Klein and non-Klein tunneling structures, *J. Appl. Phys.* **112** (2012) 073711.
39. S. V. Zhukovsky *et al.*, Spectral scalability as a result of geometrical self-similarity in fractal multilayers, *Europhys. Lett.* **66** (2004) 455–461.
40. P. Markos and C. M. Soukoulis, *Wave Propagation: From Electrons to Photonic Crystals and Left-Handed Materials* (Princeton University Press, 2008), pp. 3–10.
41. G. G. Naumis, Minimal multifractality in the spectrum of a quasiperiodic Hamiltonian, *Phys. Lett. A* **365** (2007) 171–174.
42. L. M. Gaggero-Sager *et al.*, Self-similarity in semiconductors: Electronic and optical properties, in *Optoelectronics — Materials and Techniques*, ed. P. Predeep (InTech, 2011), pp. 435–458, Available at: http://www.intechopen.com/books/optoelectronics-materials-and-techniques/self-similarity-in-semiconductors-electronic-and-optical-properties.
43. M. I. Katsnelson *et al.*, Chiral tunnelling and the Klein paradox in graphene, *Nat. Phys.* **2** (2006) 620–625.
44. D. S. Diaz-Guerrero *et al.*, Transmittance and fractality in a Cantor-like multibarrier system, *Prog. Electromagn. Res. Lett.* **2** (2008) 149–155.